Magnetic, thermodynamic, electronic, and transport properties of $CeNi_4Al$

T. Toliński,[1] A. Kowalczyk,[1] G. Chełkowska,[2] M. Pugaczowa-Michalska,[1] B. Andrzejewski,[1] V. Ivanov,[3] A. Szewczyk,[4] and M. Gutowska[4]

[1]*Institute of Molecular Physics, Polish Academy of Sciences, Smoluchowskiego 17, 60-179 Poznań, Poland*

[2]*Institute of Physics, Silesian University, Uniwersytecka 4, 40-007 Katowice, Poland*

[3]*General Institute of Physics, RAS, Vavilov 38, Moscow, Russia*

[4]*Institute of Physics, Polish Academy of Sciences, Al. Lotników, 02-668 Warszawa, Poland*

(Received 10 January 2004; revised manuscript received 18 May 2004; published 20 August 2004)

The $CeNi_4Al$ compounds have been studied using the magnetic susceptibility, specific heat, electrical resistivity and x-ray photoemission spectroscopy (XPS) measurements. The XPS experiments were supported by the theoretical calculations employing the TB LMTO method. The estimation of the hybridization, Δ, between the f-level and the conduction states was based on the XPS measurements of the Ce($3d$) states and revealed a small value of $\Delta \approx 37$ meV accompanied by a nearly full f-occupancy ($n_f \approx 0.88$). The temperature measurements of the dc susceptibility have shown paramagnetic behavior fulfilling the Curie-Weiss law with $\mu_{\mathrm{eff}} = 0.6\mu_B$/f.u. Experimental values of the specific heat coefficient $\gamma = 29$ mJK^{-2} mol^{-1} and the Debye temperature $\theta_D = 315$ K have been obtained. The electrical resistivity measurements revealed a presence of a minimum at about 16 K.

DOI: 10.1103/PhysRevB.70.064413 PACS number(s): 75.20.Hr, 72.15.Qm, 82.80.Pv, 71.20.Eh

I. INTRODUCTION

In the series of rare earth-intermetallic ($R-I$) compounds the use of cerium as the R element is especially interesting because it can lead to such properties as the intermediate valence or Kondo effect. The intermediate valence is observed in the presence of relatively strong hybridization between the f-orbitals and the conduction states and can be extracted from x-ray photoemission spectroscopy (XPS) measurements[1–4] owing to the appearance of the additional satellites within the Ce($3d_{5/2,3/2}$) doublet. The theoretical background for the interpretation of the XPS Ce($3d$) spectra was put by Gunnarsson and Schönhammer[1] in the approximation of the single impurity Anderson Hamiltonian. The XPS studies play an important role in understanding the electronic structure of Ce-based alloys and compounds.

The second effect of interest, i.e., the Kondo behavior appears as a minimum in the temperature dependence of resistivity due to the interplay between the increasing spin-disorder resistivity and the decreasing lattice scattering during cooling down the sample. It occurs on conditions that localized magnetic moments exist in a metallic matrix, which are decoupled and the s-f direct exchange interaction integral $J_{s\text{-}f}$ is negative. Below the so called Kondo temperature T_K a Kondo system is characterized by a large magnetic susceptibility and increased electronic specific heat coefficient.[5–7]

These fundamental phenomena are still in a focus of interest because they can provide an insight into the ground state properties. Recently we have observed a mixed-valence state in $CeNi_4B$ compounds.[3] In this paper we present the results of the XPS experiment as well as the measurements of the temperature dependence of the dc magnetic susceptibility, electrical resistivity and specific heat of $CeNi_4Al$. The properties of the XPS Ce($3d$) spectrum have been analyzed within the limits of the Gunnarsson and Schönhammer (G-S) model and the valence band spectrum has been calculated employing the spin-polarized Tight Binding Linear Muffin Tin Orbital (TB LMTO) method in the atomic sphere approximation (ASA).[8] We provide first such extended studies of this compound employing four different experimental methods and theoretical calculations of the electronic structure. $CeNi_4Al$ belongs to the RNi_4X (R = rare earth, X = B, Al) series exhibiting a wide range of interesting fundamental properties like large anisotropy, superconductivity, mixed-valency, etc. The RNi_4Al materials have attracted attention after successful commercial use of the $LaNi_5$ alloys in batteries and for hydrogen storage due to the large hydrogen absorption.[9,10]

II. EXPERIMENT

The polycrystalline $CeNi_4Al$ compounds were synthesized by the induction melting under an argon atmosphere. As the ingot a stoichiometric amounts of the Ce, Ni and Al were used. The crystallographic structure is of the hexagonal $CaCu_5$-type, space group $P6/mmm$. Ce occupies the $1a$ site (0,0,0) and Ni(1) the $2c$ site $(1/3,2/3,0)$. Ni(2) and Al are statistically distributed on the $3g$ site $(1/2,0,1/2)$. The structure was verified by x-ray diffraction studies using Cu Kα radiation ($\lambda = 1.5418$ Å). Figure 1 shows the profile analysis carried out with FULLPROF. The resulting lattice constants are $a = 4.953$ Å and $c = 4.089$ Å. The analysis of the x-ray data confirms that the studied samples are single phase.

The XPS experiments were performed at the photon energy of 1487.6 eV with the energy resolution of 0.3 eV. An Al-Kα source was employed using a PHI 5700/660 Physical Electronics Spectrometer. The samples were broken and measured in a vacuum of 10^{-10} Torr.

Measurements of the dc susceptibility in a magnetic field up to 9 T and temperature down to 4.2 K were carried out on a MagLab2000 instrument.

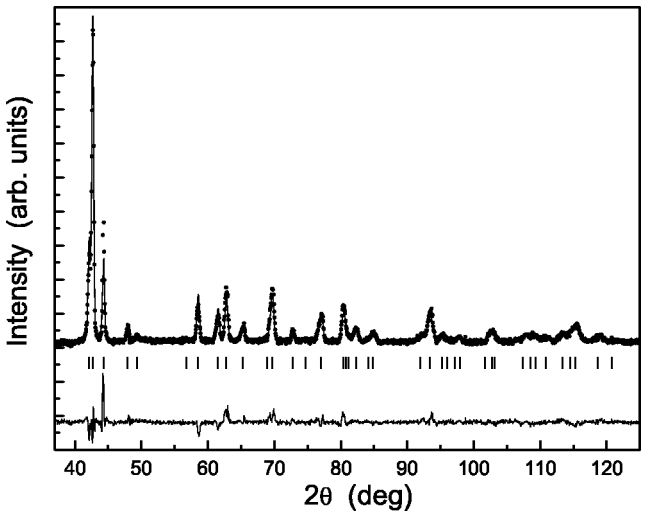

FIG. 1. X-ray diffraction pattern measured (points) for $CeNi_4Al$. A solid line presents the profile refinement using FULLPROF. The bottom solid line shows the difference between the measured and calculated pattern. The ticks indicate the position of the structural reflections.

The electrical measurements were carried out by a standard four-probe technique on a rectangular-shaped sample for a correct determination of the sample resistivity.

The specific heat was measured using a calorimeter enabling measurements in the temperature range from pumped helium temperatures up to room temperature. Over the whole temperature range the quasi-adiabatic method was applied.

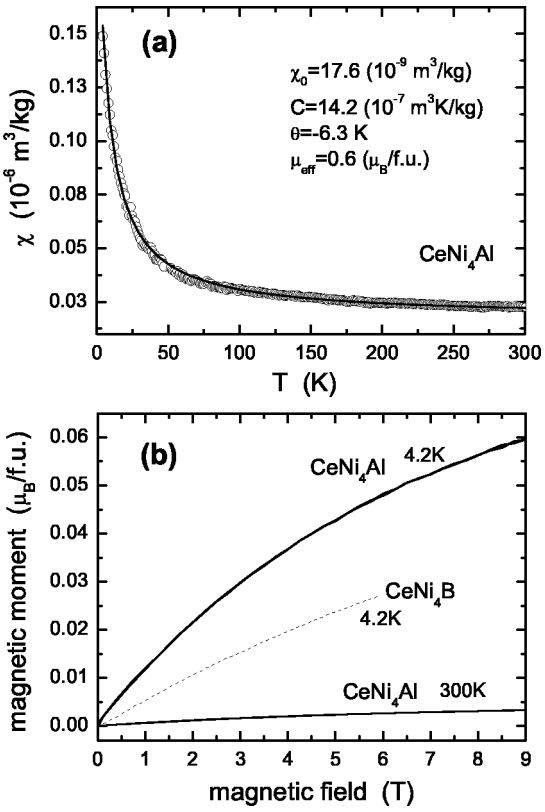

FIG. 2. (a) Temperature dependence of the dc susceptibility. Solid line: fit with the modified Curie-Weiss law. (b) $M(H)$ dependence for $CeNi_4Al$ at 4.2 K and 300 K. For a comparison the $M(H)$ dependence of $CeNi_4B$ at 4.2 K is displayed as a dashed line.

III. MAGNETIC AND THERMODYNAMIC PROPERTIES

Our previous magnetic, neutron diffraction and XPS studies of the RNi_4Al compounds have shown that the Ni atoms in this system do not contribute any magnetic moment. Therefore, the $CeNi_4Al$ compound shows paramagnetic behavior like the previously studied $CeNi_4B$.[11] The temperature dependence of the dc susceptibility for $CeNi_4Al$ is presented in Fig. 2(a). The experimental data were fitted with the modified Curie-Weiss law $\chi(T)=\chi_0+C/(T-\theta)$, which provided very similar values of the parameters as in the case of $CeNi_4B$. We have obtained $\chi_0=17.6\times10^{-9}\ \mathrm{m^3/kg}$, $\theta=-6.2$ K and $C=14.2\times10^{-7}\ \mathrm{m^3K/kg}$, whereas for $CeNi_4B$ the values were $\chi_0=16.6\times10^{-9}\ \mathrm{m^3/kg}$, $\theta=-10.7$ K and $C=11\times10^{-7}\ \mathrm{m^3K/kg}$.[11] The effective magnetic moment is $\mu_{\mathrm{eff}}=0.6\mu_B$/f.u., which is slightly larger than for $CeNi_4B$ ($\mu_{\mathrm{eff}}=0.52\mu_B$/f.u.). The increased magnetic susceptibility is also confirmed by the magnetization curve measurements. Figure 2(b) shows the $M(H)$ dependence for $CeNi_4Al$ at 4.2 K and 300 K and for a comparison the $M(H)$ dependence of $CeNi_4B$ at 4.2 K is also displayed as a dashed line. $CeNi_4Al$ exhibits a larger moment, besides, it is evident that for both compounds, but especially for $CeNi_4Al$, a small magnetic order, revealed by the curvature of the $M(H)$ line, can be induced if using high magnetic fields. They may be the Ni atoms or some minor impurities giving this effect. The curvature may be also due to the typical tendency to saturation of the Brillouin function when the ratio H/T is large and we have both low temperature (4.2 K) and relatively high magnetic fields (up to 9 T).

The larger μ_{eff} of $CeNi_4Al$ as compared with $CeNi_4B$ can be explained by the difference in the distance between the nearest Ce neighbors. $CeNi_4B$ crystallizes in the structure of $CeCo_4B$ with space group $P6/mmm$. The Ni atoms occupy the crystallographic sites $2c$ and $6c$, the rare earth is also located in two sites $1a$, $1b$, and boron atoms are located in the $2d$ positions. The lattice constants are $a=5.00$ Å and $c=6.99$ Å. The values for the $CeNi_4Al$ compound are $a=4.953$ Å and $c=4.089$ Å. However, the resulting Ce-Ce distance is $d_c=3.49$ Å in the c direction of $CeNi_4B$ and $d_c=4.089$ Å for $CeNi_4Al$. As it will be shown in Sec. IV it can be a source of a smaller hybridization effects in $CeNi_4Al$. Larger coupling between the f states and the conduction electrons leads to an increased contribution of Ce^{4+} ions having a zero magnetic moment, thus implying a smaller average value of μ. We found that $d_c(CeNi_4B)/d_c(CeNi_4Al) \approx \mu_{\mathrm{eff}}(CeNi_4B)/\mu_{\mathrm{eff}}(CeNi_4Al)$. From the G-S model[1] it is known that the hybridization parameter $\Delta \propto 1/\chi$. We have obtained larger χ and smaller Δ for $CeNi_4Al$ than for $CeNi_4B$ in accordance to this proportionality.

Our dc and ac magnetic susceptibility studies do not show an evidence of any magnetic transition, however, specific heat measurements illustrated in Fig. 3 reveal a small peak at

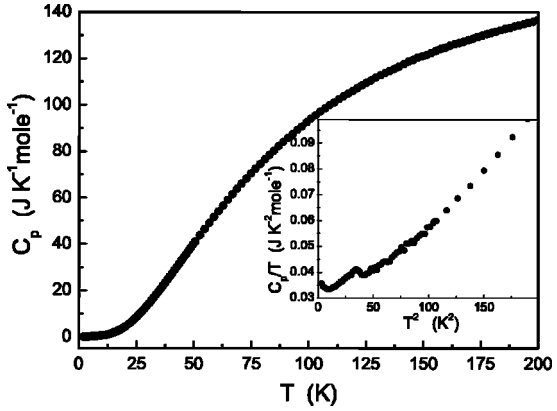

FIG. 3. Temperature dependence of the specific heat C_p. Inset: C_p/T versus square of temperature.

about 6 K (see the inset). This is developed by the crystal field induced Schottky anomaly often observed in similar compounds.

From a linear fit to the low temperature part of C_p/T versus T^2 data the electronic specific heat coefficient $\gamma = 29\ \mathrm{mJK^{-2}\,mol^{-1}}$ and the Debye temperature $\theta_D = 315$ K were extracted. The Debye temperature obtained directly from the specific heat at a given temperature, but above about 15 K, i.e., in the range were the phonon contribution dominates, increases from 275 K up to 325 K. In the case of the temperature dependence of the electrical resistivity for the isostructural nonmagnetic YNi_4Al compound we have previously obtained $\theta_D = 204$ K by fitting to the standard Bloch-Grüneisen formula.[12]

IV. XPS VALENCE BAND: CALCULATIONS AND EXPERIMENT

The electronic structure was calculated by the spin-polarized Tight Binding Linear Muffin Tin Orbital (TB LMTO) method in the atomic sphere approximation (ASA).[8] The values of the atomic sphere radii were taken in such a way that the sum of all atomic sphere volumes was equal to the volume of the unit cell. The standard combined corrections for overlapping were used to compensate for errors due to the ASA. The exchange correlation potential was assumed in the form proposed by Barth and Hedin[13] and Langreth-Mehl-Hu nonlocal corrections were included.[14] The scalar relativistic wave equation was solved. In the band calculations the initial atomic configurations were taken according to the Periodic Table of Elements. We assumed for Ce core(Xe)$+4f^1 5d^1 6s^2$, for Ni: core(Ar)$+3d^8 4s^2$, and for Al: core(Ne)$+2s^2 2p^1$. The computations were done for 512 k-points in the irreducible wedge of the first Brillouin zone.

The energy band calculations performed for $CeNi_4Al$ have shown that the paramagnetic state is more stable, because the total energy of the paramagnetic state is lower by 0.37 meV/atom than the ferromagnetic one. Hence, the calculations support the paramagnetism of $CeNi_4Al$ observed in magnetic measurements described in the previous section. The calculations show that the total and local magnetic moments are approximately zero in the ferromagnetic state. The calculated densities of states (DOS) are shown in Fig. 4. The total DOS is presented in Fig. 4(a) and the DOS for the Ce, Ni and Al atoms in the different crystallographic positions is included in Figs. 4(b)–4(d). The contribution to the DOS between 0 and 6 eV is mainly due to the Ni atoms in positions 2*c* and 3*g*. Those states are mostly occupied. The *f*-states of Ce are close to the Fermi level. The density of states for $CeNi_4Al$ is $N(E_F) = 6.7$ states $\mathrm{eV^{-1}}$/cell at the Femi level. The electronic specific heat coefficient $\gamma = (\pi k_B)^2 N(E_F)/3$ estimated from band calculations is about 15.8 $\mathrm{mJK^{-2}\,mol^{-1}}$. This value is lower then that of $CeNi_4B$ compound[3] (27.6 $\mathrm{mJK^{-2}\,mol^{-1}}$) and is roughly in agreement with the specific heat studies presented in Sec. III.

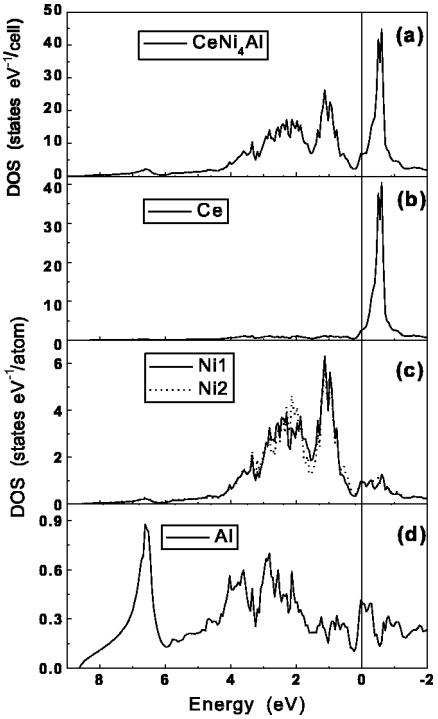

FIG. 4. The calculated total DOS (a) and the DOS for the Ce, Ni, and Al atoms in the different crystallographic positions [(b–d)].

The theoretical XPS spectrum in the region of the valence band was extracted from the DOS by weighting with appropriate atomic cross-sections and a convolution with a Lorentzian function of width 0.4 eV. In Fig. 5 we plot the calculated XPS together with the experimental data. A larger DOS at Fermi level for $CeNi_4B$ in comparison to $CeNi_4Al$ is expected because the calculated position of the Ce(4*f*) peak is closer by about 0.07 eV to E_F for the former than for the latter [Fig. 4(b)]. The shift of the valence band is also confirmed by the experimental studies because the measured XPS peak in Fig. 5 is also shifted by about 0.1 eV to the right comparing to its position for $CeNi_4B$.[3] The appearance of the 4*f* states closer to E_F suggests the possibility of larger hybridization effects for $CeNi_4B$. It is really corroborated by the XPS (3*d*) spectra analyzed in the next section.

We cannot conclude qualitatively about the DOS based on the experimentally obtained XPS valence band but some relations can be roughly compared. The ratio of the XPS in-

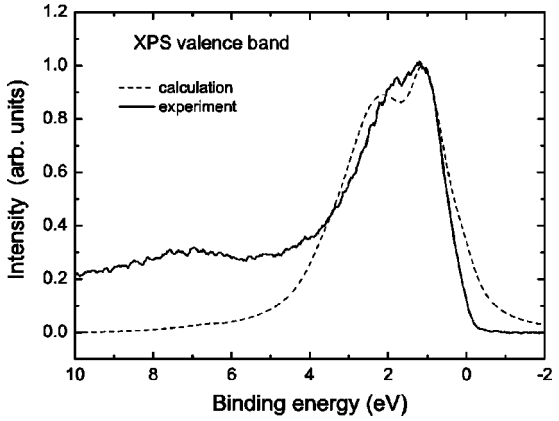

FIG. 5. The experimental and calculated XPS valence band of $CeNi_4Al$.

tensity of $CeNi_4B$ and $CeNi_4Al$ at E_F is 1.36 and the corresponding ratio of the calculated DOS is 1.45. This consistent tendency confirms the correctness of the theoretical treatment.

V. XPS OF CE(3*d*) STATES

An inherent feature of the x-ray photoemission spectroscopy is that it drives the system into an excited state. However, models like the G-S theory[1] enable drawing conclusions also about the ground state. Concerning the hybridization effects and mixed-valence behavior in the Ce-based compounds and alloys, some information can be extracted from the analysis of the Ce(3*d*) states. The appearance of the $3d^94f^0$ configuration is related to the modification of the valence state, whereas the $3d^94f^2$ satellite is a measure of the hybridization strength Δ. The measured Ce(3*d*) XPS spectrum of $CeNi_4Al$ is presented in Fig. 6 together with a decomposition performed assuming the peaks positions as in the case of the $CeNi_5$ compound.[2,15] An additional peak at 900.6 eV is due to an oxide. The $3d^94f^0$ and $3d^94f^2$ satellites are not very well pronounced, nevertheless, based on the intensity ratios $r=I(f^2)/[I(f^1)+I(f^2)]$ and r_0

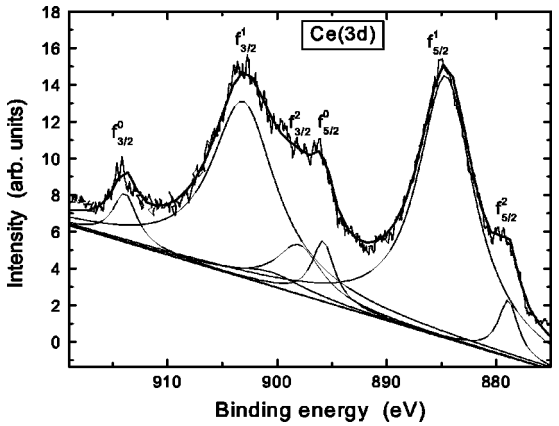

FIG. 6. Measured Ce(3*d*) XPS spectrum of $CeNi_4Al$. A decomposition is displayed assuming the peak positions as in the case of $CeNi_5$ compound.

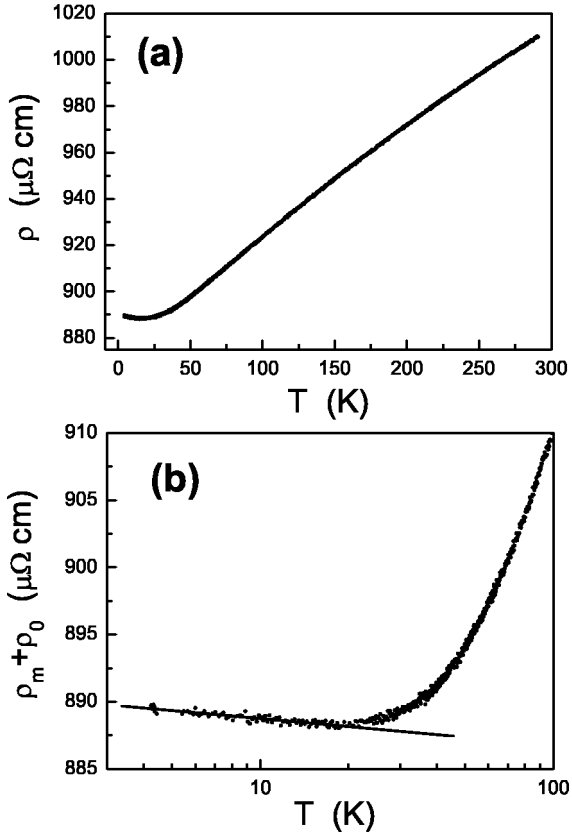

FIG. 7. (a) Temperature dependence of resistivity for the $CeNi_4Al$ compound. (b) The minimum in resistivity shown in a logarithmic scale after subtracting the phonon contribution; solid line: fit with Eq. (1).

$=I(f^0)/[I(f^0)+I(f^1)+I(f^2)]$ the hybridization parameter $\Delta \approx 37$ meV and *f*-occupancy $n_f \approx 0.88$ are roughly estimated assuming that the ratios depend on n_f and Δ in this same manner as for Ce metal.[1,2,4] These values can now be compared with our previous studies of $CeNi_4B$,[3] where we obtained $\Delta \approx 85$ meV and *f*-occupancy $n_f \approx 0.83$. A significant difference between Δ of these two compounds is evident. To explain it we recall once again the argument of the differences in the crystallographic structures of RNi_4Al and RNi_4B. The Ce-Ce distance in the *c* direction for the former is significantly larger than for the latter. It is then clear that the hybridization for $CeNi_4Al$ should be smaller than for the B-based counterpart.

VI. ELECTRICAL RESISTIVITY MEASUREMENTS

The next step of our studies on $CeNi_4Al$ compound concerns the temperature dependence of resistivity. The $\rho(T)$ curve shown in Fig. 7(a) does not reveal any transition to a different (ordered) phase, which supports additionally the results of magnetic studies described in Sec. II, as well as the prediction of the theoretical calculations with the TB LMTO method (Sec. IV) revealing a paramagnetic ground state. A total resistivity is given by the sum $\rho(T)=\rho_0+\rho_{ph}(T)+\rho_m(T)$, where ρ_0 is a residual resistivity, ρ_{ph} represents the phonon contribution and ρ_m includes the spin-disorder resis-

tivity and the spin fluctuations term. To extract the magnetic contribution a procedure described in more details elsewhere was employed,[3,12,16] i.e., the nonmagnetic YNi_4Al reference sample was fitted by the modified Bloch-Grüneisen relation for metal-like compounds and the resulting phonon contribution $\rho_{ph}(T)$ was subtracted from $CeNi_4Al$. The remaining magnetic contribution, $\rho_m+\rho_0$, as a function of temperature in the range 4.2 K–100 K is displayed in Fig. 7(b). It is evident that a minimum occurs in the temperature dependence of resistivity at about 16 K. Below this threshold the results can be described using the relation

$$\rho_{mag}(T) = \rho_0^{\infty} - \rho_K \ln T, \quad (1)$$

where the spin-disorder resisitivity $\rho_0^{\infty}=891\ \mu\Omega$cm and the coefficient $\rho_K=0.85\ \mu\Omega$cm. This formula is usually employed for Kondo systems, however, the magnetic susceptibility and the electronic specific heat coefficient do not support the presence of the Kondo effect in the studied sample. The increased ρ_0 is mainly due to the random distribution of the Ni(2) and Al on the 3*g* site as has been also observed for $NdNi_4Al$.[12]

In our previous studies of $CeNi_4B$ compound the parameters of Eq. (1) were $\rho_0^{\infty}=88.4\ \mu\Omega$cm and $\rho_K=0.29\ \mu\Omega$cm.[3,16] The minimum at $\rho(T)$ dependence was more shallow than for $CeNi_4Al$ and appeared at about 12 K, i.e., at a lower temperature.

VII. CONCLUSIONS

The TM LMTO calculations, the ac magnetic susceptibility and the specific heat measurements of the $CeNi_4Al$ compound have shown that it is a paramagnetic material. The calculation of the valence band reveals the dominance of the Ni(3*d*) states below the Fermi level and the *f* peak is about 0.56 eV above E_F. The theoretical valence band below E_F is in good agreement with the XPS measurements. The thermodynamic measurements have provided the specific heat coefficient $\gamma=29\ \mathrm{mJK^{-2}\,mol^{-1}}$, which is comparable with a theoretically calculated value of $15.8\ \mathrm{mJK^{-2}\,mol^{-1}}$. The Debye temperature is equal to 315 K. In comparison with the earlier studied $CeNi_4B$, the $CeNi_4Al$ compound is characterized by (i) a smaller DOS at E_F as results from TB LMTO calculations and a comparison of the measured XPS valence bands; (ii) a lower value of the hybridization parameter Δ as derived from the Gunnarsson-Schönhammer analysis of the Ce(3*d*) peaks. It is confirmed by a longer Ce-Ce distance in the *c* direction; (iii) a larger residual resistivity, which results from the large lattice disorder at the 3*g* site occupied randomly by Ni and Al; (iv) a better pronounced minimum in the temperature dependence of resistivity.

ACKNOWLEDGMENT

This work was supported by the Centre of Excellence for Magnetic and Molecular Materials for Future Electronics within the European Commission; Contract No. G5MA-CT-2002-04049.

[1] O. Gunnarsson and K. Schönhammer, Phys. Rev. B **28**, 4315 (1983).
[2] J. C. Fuggle, F. U. Hillebrecht, Z. Zolnierek, R. Lässer, Ch. Freiburg, O. Gunnarsson, and K. Schönhammer, Phys. Rev. B **27**, 7330 (1983).
[3] T. Toliński, A. Kowalczyk, M. Pugaczowa-Michalska, and G. Chełkowska, J. Phys.: Condens. Matter **15**, 1397 (2003).
[4] A. Ślebarski, M. Neumann, and S. Mähl, Phys. Rev. B **51**, 11 113 (1995); A. Ślebarski, E. D. Bauer, Shi Li, M. B. Maple, and A. Jezierski, *ibid.* **63**, 125126 (2001).
[5] B. Coqblin *et al.*, in Frontiers in *Solid State Sciences, Selected Topics in Magnetism*, edited by L. C. Gupta and M. S. Multani, (World Scientific, Singapore, 1993), Vol. 2, p.75.
[6] H. Michor, St. Berger, M. El-Hagary, C. Paul, E. Bauer, G. Hilscher, P. Rogl, and G. Giester, Phys. Rev. B **67**, 224428 (2003).
[7] H. von Löhneysen, J. Clin. Eng. **8**, 9689 (1996).
[8] O. K. Andersen, O. Jepsen, and M. Sob, in *Electronic Band Structures and Its Applications*, Springer Verlag Lecture Notes in Physics, edited by M. Yussouff (Springer-Verlag, Berlin, 1987), Vol. 283, p. 1.
[9] E. L. Houston and G. D. Sandrock, J. Less-Common Met. **74**, 435 (1980).
[10] M. Wada, Sci. Technol. Jpn. **51**, 54 (1994).
[11] T. Toliński, A. Kowalczyk, A. Szlaferek, M. Timko, and J. Kováč, Solid State Commun. **122**, 363 (2002).
[12] T. Toliński, W. Schäfer, W. Kockelmann, A. Kowalczyk, and A. Hoser, Phys. Rev. B **68**, 144403 (2003).
[13] U. von Barth and L. Hedin, J. Phys. C **5**, 1629 (1972).
[14] C. D. Hu and D. C. Langreth, Phys. Scr. **32**, 391 (1985).
[15] T. Toliński, A. Kowalczyk, and G. Chełkowska, Phys. Lett. A **308**, 75 (2003).
[16] T. Toliński, A. Kowalczyk, and V. Ivanov, Phys. Status Solidi B **240**, 153 (2003).